

Cite this: *Dalton Trans.*, 2024, **53**,
14897

Synthesis and properties of metal trifluoride complexes with amide-functionalised tacn macrocycles and radiofluorination of $[\text{GaF}_3(\text{L}^1)]$ by $^{18}\text{F}/^{19}\text{F}$ isotopic exchange†

Charley O'Callaghan,^a Victoria K. Greenacre,^a Rhys P. King,^a Julian Grigg,^b
Julie M. Herniman,^a Graeme McRobbie^b and Gillian Reid^{a*}

Three amide-functionalised tacn macrocyclic derivatives (tacn = 1,4,7-triazacyclononane) are reported, two tris-amide derivatives, L^1 containing three $-\text{CH}_2\text{C}(\text{O})\text{NHPh}$ pendant arms, L^2 containing three $-\text{CH}_2\text{CH}_2\text{C}(\text{O})\text{NH}^i\text{Pr}$ pendant arms, and one *mono*-amide, L^3 , containing ^iPr groups on two of the tacn amine functions and a single $-\text{CH}_2\text{C}(\text{O})\text{NHPh}$ function on the third. The reactions of these new ligands towards $[\text{MF}_3(\text{dmsO})(\text{OH}_2)_2]$ ($\text{M} = \text{Al}, \text{Ga}$) and towards $\text{FeF}_3 \cdot 3\text{H}_2\text{O}$ in alcoholic solution afford the complexes $[\text{MF}_3(\text{L})]$ ($\text{L} = \text{L}^1-\text{L}^3$) in good yields as powdered solids. These complexes are characterised by IR and multinuclear NMR spectroscopy (diamagnetic species only) and mass spectrometry. $[\text{GaF}_3(\text{L}^1)]$, $[\text{GaF}_3(\text{L}^3)]$ and $[\text{FeF}_3(\text{L}^3)]$ are also characterised by single crystal X-ray analysis. The corresponding reactions involving $[\text{InF}_3(\text{dmsO})(\text{OH}_2)_2]$ yield mixtures of products (along with F^-), consistent with the M–F bond strengths decreasing as group 13 is descended. A few crystals of the target complex, $[\text{InF}_3(\text{L}^2)]$, were also obtained from one such reaction. All of the complexes adopt *fac*-octahedral coordination *via* the amine N-donor atoms and retain the three fluoride ligands both in solution and in the solid state. Extensive intramolecular hydrogen-bonding involving the amide NH pendant groups and the MF_3 moieties is evident in the crystal structures. In the isostructural $[\text{MF}_3(\text{L}^3)]$ ($\text{M} = \text{Ga}, \text{Fe}$) complexes the head-to-tail $\text{C}(\text{O})\text{NH}\cdots\text{F}$ H-bonded dimers observed in the solid state resemble those found frequently in organic compounds and that form the cornerstone of many supramolecular assemblies. This is consistent with the MF_3 fragments being strong H-bond acceptors. Radiofluorination of $[\text{GaF}_3(\text{L}^1)]$ by $^{18}\text{F}/^{19}\text{F}$ isotopic exchange in MeOH at $3 \mu\text{mol mL}^{-1}$ precursor concentration and using aqueous $^{18}\text{F}\text{F}^-$ in target water (75% : 25%) with gentle heating (80 °C, 10 min) gave *ca.* 20% radiochemical yield of $[\text{Ga}^{18}\text{FF}_2(\text{L}^1)]$. In contrast, no ^{18}F incorporation occurs with $[\text{GaF}_3(\text{L}^3)]$ under any of the conditions explored.

Received 18th July 2024,
Accepted 20th August 2024
DOI: 10.1039/d4dt02074j
rsc.li/dalton

Introduction

The last decade has seen considerable research into new metal–fluoride complexes, much of which has been motivated by their potential as carriers for the positron-emitting ^{18}F radioisotope for positron emission tomography (PET) imaging in medicine.^{1–3} In selecting the target metal complexes, key

requirements are that the metal–fluoride bond is sufficiently strong to allow easy and fast incorporation of the radiofluorine at a late stage in the procedure and for the radiolabelled complex to be stable to hydrolysis/substitution/decomposition under physiological conditions. Towards this objective, several systems incorporating aluminium(III), gallium(III), iron(III) and scandium(III) fluoride species bound to neutral^{4–7} or anionic^{8–12} tacn-based ligands (tacn = 1,4,7-triazacyclononane) have been reported.

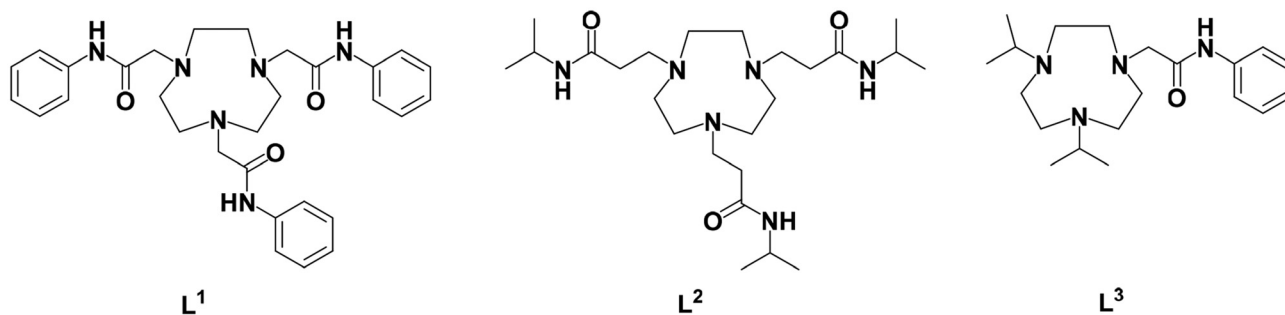
Notably, the $[\text{MF}_3(\text{L})]$ ($\text{L} = \text{Me}_3\text{-tacn}$, $\text{BnMe}_2\text{-tacn}$, 1,4,7-tris(2-amino-3,5-di-*tert*-butylbenzyl)-1,4,7-triazacyclononane) complexes frequently form extended H-bonding networks with lattice water or MeOH molecules *via* $\text{F}\cdots\text{HOH}$ or $\text{F}\cdots\text{HOCH}_3$ interactions.^{13,14} These complexes can also function as metal-ligands towards Lewis acids such as Gd^{3+} ¹⁵ and alkali metal cations, as well as $[\text{NH}_4]^+$.¹⁶ We were therefore interested in expanding the coordination chemistry of these ‘ MF_3 ’ frag-

^aSchool of Chemistry, University of Southampton, Southampton SO17 1BJ, UK.
E-mail: G.Reid@soton.ac.uk

^bGE HealthCare, Pollards Wood, Nightingales Lane, Chalfont St Giles, Bucks, HP8 4SP, UK

† Electronic supplementary information (ESI) available: NMR, IR and mass spectra associated with ligands L^1-L^3 and the metal trifluoride complexes described in this work (Fig. S1–S17), together with the crystal structure of $\text{L}^1\text{-HNO}_3$, CCDC 2355936–2355941. For ESI and crystallographic data in CIF or other electronic format see DOI: <https://doi.org/10.1039/d4dt02074j>





Scheme 1 The amide functionalised tacn ligands, L^1 – L^3 , employed in this work.

ments ($M = \text{Al}, \text{Ga}, \text{In}, \text{Fe}$) with tacn-derivatives carrying pendant H-bond donor functions, since these may be relevant in facilitating the delivery of highly electronegative fluoride ions to the metal in the course of radiofluorination, and may also lead to unusual inorganic H-bonded assemblies in the final complexes.

A plethora of tacn-derivatives with pendant arm functions is known. In considering possible H-bond donor pendant functions, amide groups were selected since these frequently feature in bioconjugates in medical imaging agents, for example, through coupling of a pendant carboxylic acid group to a peptide-based amine function and are therefore generally biocompatible.¹⁷

Several amide-functionalised tacn ligands have been reported in the literature and their coordination chemistry with (mostly) divalent metal salts described.^{18–23} Of these, the tris(amide)-tacn ligands typically function as hexadentate chelators *via* the three macrocyclic amine donor atoms and the three carboxamide oxygen atoms (N_3O_3 donor set), affording distorted octahedral dicationic metal species, that can be isolated with non-coordinating (*e.g.* nitrate, perchlorate or tetrafluoroborate) anions.

In the present study we describe the coordination of pyramidal ‘ MF_3 ’ fragments towards both *mono*- and *tris*(amide)-functionalised tacn ligands, L^1 – L^3 , specifically with a view to utilising the macrocycle as a neutral N_3 -donor ligand, intentionally leaving the pendant amide group(s) uninvolved in the metal coordination sphere and available as potential H-bond donor group(s). The synthesis and spectroscopic characterisation of L^1 – L^3 (Scheme 1) derived from the nine-membered tacn (1,4,7-triazacyclononane) core are reported, L^1 and L^2 contain different linkers ($-\text{CH}_2\text{C}(\text{O})\text{NHPh}$ and $-\text{CH}_2\text{CH}_2\text{C}(\text{O})\text{NH}^i\text{Pr}$), while L^3 contains a single $-\text{CH}_2\text{C}(\text{O})\text{NHPh}$ pendant group.

We then explored their coordination towards various ‘ MF_3 ’ fragments ($M = \text{Al}, \text{Ga}, \text{In}, \text{Fe}$), using spectroscopic and crystallographic data to probe how the amide groups influence their molecular and extended structures, all of which are based upon *fac*-octahedral geometries with N_3F_3 donor sets at the metal, leaving the amide pendant arms uncoordinated. Single crystal X-ray structures for $L^1\cdot\text{HCl}$, $L^1\cdot\text{HNO}_3$, along with four representative metal complexes, $[\text{GaF}_3(L^1)]\cdot 1.5\text{MeOH}\cdot 0.5\text{H}_2\text{O}$,

$[\text{InF}_3(L^2)]$, $[\text{GaF}_3(L^3)]$ and $[\text{FeF}_3(L^3)]$, are reported, and the role of the H-bond donor amide groups in the solid state structures discussed. Experiments aimed at radiofluorination of the Ga(III) complexes containing L^1 and L^3 *via* $^{18}\text{F}/^{19}\text{F}$ isotopic exchange are also discussed.

Experimental

Infrared spectra were recorded as Nujol mulls between CsI plates using a PerkinElmer Spectrum 100 spectrometer over the range 4000 – 200 cm^{-1} . ^1H , $^{13}\text{C}\{^1\text{H}\}$, $^{19}\text{F}\{^1\text{H}\}$, ^{27}Al and ^{71}Ga NMR spectra were recorded from CD_3OD solutions (unless otherwise stated) using a Bruker AV400 spectrometer and referenced to SiMe_4 *via* the residual solvent resonance (^1H and ^{13}C), external CFCl_3 (^{19}F), aqueous $[\text{Al}(\text{H}_2\text{O})_6]^{3+}$ (^{27}Al) and aqueous $[\text{Ga}(\text{H}_2\text{O})_6]^{3+}$ (^{71}Ga), respectively. Low resolution mass spectra were obtained in MeOH by positive ion electrospray MS using a Waters (Manchester, UK) Acquity TQD tandem quadrupole mass spectrometer. Samples were introduced to the mass spectrometer *via* an Acquity H-Class quaternary solvent manager (with TUV detector at 254 nm , sample and column manager). Ultra-high performance liquid chromatography was undertaken using Waters BEH C18 column ($50\text{ mm} \times 2.1\text{ mm}$, $1.7\text{ }\mu\text{m}$). Gradient elution from 20% acetonitrile/80% water (0.2% formic acid) to 100% acetonitrile (0.2% formic acid) was performed over five min at a flow rate of 0.6 mL min^{-1} . High resolution positive ion electrospray mass spectra were recorded using a Maxis (Bruker Daltonics, Bremen, Germany) time of flight (TOF) mass spectrometer. Samples were infused into the ion source using a syringe driver at a constant flow rate of $3\text{ }\mu\text{L min}^{-1}$. Duplicate microanalyses were undertaken at Medac Ltd, with the majority of measurements within $\pm 0.4\%$ of the theoretical value. However, in a few cases the values are slightly outside this range, reflecting the inherent variability of microanalytical measurements across different facilities.²⁴ The purification of ligands L^1 and L^3 used a Biotage Selekt flash chromatography system (reverse-phase Sfar C18 column).

All preparations were carried out under atmospheric conditions. Reagents $\text{FeF}_3\cdot 3\text{H}_2\text{O}$ and $\text{InF}_3\cdot 3\text{H}_2\text{O}$ (Sigma-Aldrich), $\text{GaF}_3\cdot 3\text{H}_2\text{O}$ (Strem Chemicals) and $\text{AlF}_3\cdot 3\text{H}_2\text{O}$ (Alfa Aesar) were used as received. 1,4,7-Triazacyclononane (tacn),²⁵ and 1,4-dii-



sopropyl-1,4,7-triazacyclononane ($^i\text{Pr}_2\text{-tacn}$)²⁶ were synthesised as described in the literature. The 2-chloro-*N*-phenylacetamide was synthesised as described in the literature and recrystallised from $\text{CH}_2\text{Cl}_2/\text{hexane}$ before use.²⁷ *N*-Isopropylacrylamide (Sigma-Aldrich) was used as supplied. The metal precursor complexes, $[\text{MF}_3(\text{dmsO})(\text{OH}_2)_2]$ ($\text{M} = \text{Al}, \text{Ga}, \text{In}$), were prepared using the methods reported.²⁸

Ligand preparations

L¹: Tacn (0.506 g, 3.92 mmol) was added to a rapidly stirring mixture of K_2CO_3 (6.50 g, 47.0 mmol) in acetone (80 mL) in a 250 mL round bottomed flask equipped with magnetic stirring. This was stirred for 10 min at room temperature. A solution of 2-chloro-*N*-phenylacetamide (2.00 g, 11.8 mmol, 3 mol. eq.) in acetone (40 mL) was then added dropwise and the reaction mixture stirred at room temperature overnight. The resulting yellow mixture was filtered and 1.5 M NaOH (*ca.* 150 mL) was added. This solution was extracted with CHCl_3 (3 × 150 mL) and the organic extracts were combined. The solvent was removed using a rotary evaporator to leave a tan coloured oil. This was subsequently purified by flash chromatography. The crude ligand **L¹** was dissolved in a minimal volume of CHCl_3 and four mass equivalents of silica was added to the solution, creating a slurry. The CHCl_3 solvent was removed by rotary evaporation to leave a free-flowing orange powder. This was dry-loaded onto the Biotage (gradient = 40%–60% $\text{H}_2\text{O}/\text{MeCN}$ each containing 0.01% formic acid, over 4 column volumes where: CV = 164 mL and flow rate = 50 mL min⁻¹). The fractions corresponding to **L¹** were combined and the solvent was removed *in vacuo*. The residue was washed with fresh MeCN, causing precipitation of a white solid, which was collected by filtration and dried. Yield: 1.96 g, 3.53 mmol (90%). ¹H NMR (298 K, CD_3OD): δ (ppm) = 8.54 (s, **NH**), 7.50–7.46 (m, [6H], **ArH**), 7.03–6.94 (m, [9H], **ArH**), 4.85 (s, H_2O), 3.87 (br s, [6H], **CH₂**), 3.14 (br s, [12H], **tacn-CH₂**). ¹³C {¹H} NMR (298 K, CD_3OD): δ (ppm) = 169.5 (**C=O**), 139.4 (**ArC**), 129.8 (**ArC**), 125.4 (**ArC**), 121.4 (**ArC**), 59.5 (**CH₂**), 51.1 (**tacn-CH₂**). ¹³C 135-DEPT NMR (298 K, CD_3OD): δ (ppm) = 129.6 (**ArC**), 125.1 (**ArC**), 121.1 (**ArC**), 59.2 (**CH₂**), 50.9 (**tacn-CH₂**). HR ESI⁺ MS (CH_3OH): found: m/z = 529.2921 [**L¹** + H]⁺ (calculated for $[\text{C}_{30}\text{H}_{37}\text{N}_6\text{O}_3]^+$: m/z = 529.2927); 551.2738 [**L¹** + Na]⁺ (calculated for $[\text{C}_{30}\text{H}_{36}\text{N}_6\text{NaO}_3]^+$: m/z = 551.2747). IR (Nujol, ν/cm^{-1}): 3344 m, 3180 w (**NH**), 1682 s, 1596 s (**C=O**).

L¹·HCl: **L¹** was converted to its HCl salt for X-ray structure analysis. One drop of 12 M HCl was added to a solution of **L¹** (0.01 g, 0.019 mmol) in deuterated methanol (2 mL). Crystals suitable for X-ray diffraction were grown *via* slow evaporation of solvent over a period of four weeks in the fridge. ¹H NMR (298 K, CD_3OD): δ (ppm) = 8.09 (s, **NH**), 7.56–7.53 (m, [6H], **ArH**), 7.25–7.21 (m, [6H], **ArH**), 7.10–7.06 (m, [3H], **ArH**), 5.03 (s, H_2O), 4.23 (br s, [6H], **CH₂**), 3.66 (br s, [12H], **tacn-CH₂**). ¹³C {¹H} NMR (298 K, CD_3OD): δ (ppm) = 167.8 (**C=O**), 139.0 (**ArC**), 130.0 (**ArC**), 126.0 (**ArC**), 121.6 (**ArC**), 59.9 (**CH₂**), 52.9 (**tacn-CH₂**).

L²: Tacn (0.650 g, 5.03 mmol) and *N*-isopropylacrylamide (1.74 g, 15.3 mmol, 5% mol excess) were placed into a 250 mL

round bottomed flask equipped with magnetic stirring and a reflux condenser and degassed MeOH (100 mL) was added. The mixture was heated at reflux for 18 h. The resulting pale-yellow solution was filtered through Celite to remove any particulates, and the volatiles were then removed *via* rotary evaporation, leaving a pale-yellow oil. This was dissolved in 1.0 M HCl (20.5 mL) and extracted with CHCl_3 (3 × 50 mL) to remove the excess *N*-isopropylacrylamide. The organic phases were discarded. The pH of the remaining aqueous phase was adjusted to >12 using 2 M KOH (50 mL) and extracted with 3 × 50 mL CHCl_3 . The combined organic extracts were dried over MgSO_4 , filtered, and the volatiles removed *via* rotary evaporation. This left the product as a viscous yellow oil. Yield: 2.01 g, 4.46 mmol (89%). ¹H NMR (298 K, CD_3OD): δ (ppm) = 4.85 (s, H_2O), 3.98–3.92 (septet, ³ $J_{\text{H-H}} = 6.5$ Hz, [3H], **¹Pr-CH**), 3.01–2.87 (br m, [6H], **CH₂**), 2.83 (br s, [12H], **tacn-CH₂**), 2.38–2.34 (br t, [6H], **CH₂**), 1.14 (d, ³ $J_{\text{H-H}} = 6.6$ Hz, [18H], **¹Pr-CH₃**). ¹H NMR (298 K, CDCl_3): δ (ppm) = 6.72 (br, [3H], **NH**), 4.11–4.01 (septet, ³ $J_{\text{H-H}} = 6.6$ Hz, [3H], **¹Pr-CH**), 2.81–2.78 (t, ³ $J_{\text{H-H}} = 6.5$ Hz, [6H], **CH₂**), 2.76 (s, [12H], **tacn-CH₂**), 2.29–2.26 (t, ³ $J_{\text{H-H}} = 6.5$ Hz, [6H], **CH₂**), 1.14 (d, ³ $J_{\text{H-H}} = 6.6$ Hz, [18H], **¹Pr-CH₃**). ¹³C {¹H} NMR (298 K, CDCl_3): δ (ppm) = 171.3 (**C=O**), 55.6 (**tacn-CH₂**), 54.8 (**CH₂**), 41.0 (**¹Pr-CH**), 34.3 (**CH₂**), 22.9 (**¹Pr-CH₃**). ¹³C DEPT-135 NMR (298 K, CDCl_3): δ (ppm) = 55.4 (**tacn-CH₂**), 54.6 (**CH₂**), 40.8 (**¹Pr-CH**), 34.1 (**CH₂**), 22.7 (**¹Pr-CH₃**). HR ESI⁺ MS (CH_3OH): found: m/z = 491.3683 [**L²** + Na]⁺ (calculated: m/z = 491.3680), 469.3863 [**L²** + H]⁺ (calculated for $[\text{C}_{24}\text{H}_{49}\text{N}_6\text{O}_3]^+$: m/z = 469.3861), 356.3019 [**¹PrC(O)NH(CH₂)₂**]₂-tacn + H]⁺ (calculated for $[\text{C}_{18}\text{H}_{37}\text{N}_5\text{O}_2]^+$: m/z = 356.30), 235.1967 [**L²** + 2H]²⁺ (calculated for $[\text{C}_{24}\text{H}_{50}\text{N}_6\text{O}_3]^{2+}$: m/z = 235.1967). IR (neat film, ν/cm^{-1}): 3460 br, 3287 br (**OH**), 3078 br (**NH**), 1644 vs, 1554 s (**C=O**).

L³·HCl: In a 100 mL round bottomed flask equipped with magnetic stirring, $^i\text{Pr}_2\text{-tacn}$ (4.50 g, 21.1 mmol) was dissolved in degassed acetone (100 mL). Powdered K_2CO_3 (4.50 g, 32.5 mmol) was added. This was stirred at room temperature for 15 min and 2-chloro-*N*-phenylacetamide (3.57 g, 21.1 mmol) dissolved in degassed acetone (100 mL) was then added dropwise. The reaction mixture was stirred at room temperature overnight. After filtering through Celite, the filtrate was adjusted to pH 12 using aqueous 1.5 M NaOH (*ca.* 200 mL). This was extracted with 3 × 200 mL CHCl_3 , and the organic phases collected and combined. The solvent was removed *via* rotary evaporation to leave a tan-coloured oil. This crude product was purified in batches by flash chromatography using a Biotage Selekt flash chromatography system (dry-loaded; gradient = 30%–40% $\text{H}_2\text{O}/\text{MeCN}$ each containing 0.01% formic acid, over 4 column volumes where: CV = 164 mL and flow rate = 50 mL min⁻¹). A portion of the crude product (3.00 g) was dissolved in a minimal amount of CHCl_3 . Then, four mass equivalents of chromatography-grade silica was added to the solution, creating a tan-coloured slurry. The CHCl_3 solvent was removed *via* the rotary evaporator to leave a free-flowing orange powder. The pure fractions containing **L³·HCl** were collected, and the solvent was removed *in vacuo* leaving a viscous tan-coloured oil. After washing with MeCN



and further drying, the product was isolated as the protonated ligand salt, $L^3 \cdot HCl$. Yield = 2.50 g. 1H NMR (298 K, CD_3OD): δ (ppm) = 8.32 (s, NH), 7.59–7.55 (m, [2H], ArH), 7.32–7.28 (m, [2H], ArH), 7.10–7.06, 4.90 (H₂O), 3.59 (s, [2H], CH₂), 3.35 (septet, [2H], ¹Pr-CH), 3.10–3.03 (br m, [4H], tacn-CH₂), 2.96–2.87 (br m, [4H], tacn-CH₂), 2.84–2.74 (br m, [4H], tacn-CH₂), 1.25 (br d, [12H], ¹Pr-CH₃). $^{13}C\{^1H\}$ NMR (298 K, CD_3OD): δ (ppm) = 167.4 (C=O), 139.9 (ArC), 130.0 (ArC), 125.3 (ArC), 121.1 (ArC), 58.5 (CH₂), 55.3 (¹Pr-CH), 50.3 (tacn-CH₂), 48.3 (tacn-CH₂), 46.3 (tacn-CH₂), 18.4 (¹Pr-CH₃), 18.1 (¹Pr-CH₃). 135-DEPT ^{13}C NMR (298 K, CD_3OD): δ (ppm) = 129.7 (ArC), 125.0 (ArC), 120.8 (ArC), 58.2 (CH₂), 55.0 (¹Pr-CH), 50.0 (tacn-CH₂), 48.0 (tacn-CH₂), 46.0 (tacn-CH₂), 18.1 (¹Pr-CH₃), 17.8 (¹Pr-CH₃). HR ESI⁺ MS (CH₃OH): found: m/z = 347.2812 [$L^3 + H$]⁺ (calculated for $[C_{20}H_{35}N_4O]^+$: m/z = 347.2805).

$L^3 \cdot L^3 \cdot HCl$ (2.20 g, 5.74 mmol) was treated with a solution of NEt_3 (20% by volume in deionised water) until pH > 12 (ca. 150 mL). A white precipitate formed initially, which then dissolved, and an orange oil was deposited. $CHCl_3$ (100 mL) was added to dissolve the oil and the organic phase was separated and retained. Removal of the $CHCl_3$ solvent *in vacuo* yielded a tan-coloured oil. Addition of pentane (25 mL) produced a dark-yellow solution, leaving a small amount of brown residue, which was discarded. The pentane was removed *in vacuo*, leaving the final product as a dark yellow oil (1.10 g, 55%). 1H NMR (298 K, CD_3OD): δ (ppm) = 7.56–7.53 (m, [2H], ArH), 7.35–7.29 (m, [2H], ArH), 7.13–7.08 (m, [1H], ArH), 4.85 (H₂O), 2.91 (s, [2H], CH₂), 3.35 (septet, ³J_{H-H} = 6.6 Hz, [2H], ¹Pr-CH), 2.86 (s, [4H], tacn-CH₂), 2.75–2.70 (br m, [8H], tacn-CH₂), 0.95 (d, ³J_{H-H} = 6.6 Hz, [12H], ¹Pr-CH₃). $^{13}C\{^1H\}$ NMR (298 K, CD_3OD): δ (ppm) = 173.6 (C=O), 139.4 (ArC), 129.8 (ArC), 125.4 (ArC), 121.5 (ArC), 62.9 (CH₂), 59.8 (tacn-CH₂), 56.0 (¹Pr-CH), 18.3 (¹Pr-CH₃). 135-DEPT ^{13}C NMR (298 K, CD_3OD): δ (ppm) = 129.9 (ArC), 125.5 (ArC), 121.7 (ArC), 63.0 (CH₂), 59.9 (tacn-CH₂), 56.1 (¹Pr-CH), 49.7 (tacn-CH₂), 18.4 (¹Pr-CH₃). 1H NMR (298 K, $CDCl_3$): δ (ppm) = 10.84 (s, [1H], NH), 7.59–7.56 (m, [2H], ArH), 7.34–7.28 (m, [2H], ArH), 7.11–7.05 (m, [1H], ArH), 3.37 (s, [2H], CH₂), 2.88 (septet, ³J_{H-H} = 6.1 Hz [2H], ¹Pr-CH), 2.82 (br s, [4H], tacn-CH₂), 2.70 (br s, [8H], tacn-CH₂), 1.56 (H₂O), 0.93 (d, ³J_{H-H} = 6.6 Hz, [12H], ¹Pr-CH₃). $^{13}C\{^1H\}$ NMR (298 K, $CDCl_3$): δ (ppm) = 171.3 (C=O), 139.6 (ArC), 128.7 (ArC), 123.7 (ArC), 119.9 (ArC), 62.5 (CH₂), 59.4 (tacn-CH₂), 55.8 (¹Pr-CH), 54.9 (tacn-CH₂), 49.1 (tacn-CH₂), 18.0 (¹Pr-CH₃). HR ESI⁺ MS (CH₃OH): found: m/z = 347.2812 [$L^3 + H$]⁺ (calculated for $[C_{20}H_{35}N_4O]^+$: m/z = 347.2805). IR (neat film, ν/cm^{-1}): 3400 br, 3200 br (OH), 3053, 3033 w (NH), 2961, 2930, 2812 (C–H stretch), 1678 br s, 1600 (C=O).

Metal trifluoride complexes

$[AlF_3(L^1)]$. A solution of $[AlF_3(dmsO)(OH_2)_2]$ (0.011 g, 0.057 mmol) in MeOH (5 mL) was added to a solution of L^1 (0.030 g, 0.057 mmol) in MeOH (5 mL). This was stirred at room temperature overnight, during which time a white precipitate had formed. This was separated from the reaction solution *via* filtration. The solvent volume was then reduced to approx. 2 mL *in vacuo* and diethyl ether (20 mL) was added,

causing precipitation of a white solid. This was filtered and dried *in vacuo*. Yield: 0.027 g, 0.035 mmol (62%). Anal. required for $C_{30}H_{36}AlF_3N_6O_3 \cdot 2dmsO$: C, 53.11; H, 6.29; N, 10.93. Found: C, 51.30; H, 6.13; N, 11.24%. 1H NMR (CD_3OD , 298 K): δ (ppm) = 7.50–7.48 (m, [6H], ArH), 7.03–6.94 (m, [9H], ArH), 4.85 (H₂O), 3.87 (s, [6H], CH₂), 3.21–3.09 (br m, [12H], tacn-CH₂), 2.66 (dmsO). $^{19}F\{^1H\}$ NMR (CD_3OD , 298 K): δ (ppm) = –174.1 (br s). $^{13}C\{^1H\}$ NMR (CD_3OD , 298 K): δ (ppm) = 168.5 (C=O), 139.4 (ArC), 129.8 (ArC), 125.4 (ArC), 121.4 (ArC), 59.5 (CH₂), 51.1 (tacn-CH₂), 40.6 (dmsO). HR ESI⁺ MS (CH₃OH): found: 529.2934 [$L^1 + H$]⁺ (calculated: m/z = 529.2927), 551.2744 [$L^1 + Na$]⁺ (calculated: m/z = 551.2747), 613.2666 [$AlF_3(L^1) + H$]⁺ (calculated: m/z = 613.2689). IR (Nujol, ν/cm^{-1}): 3450 br, 3300 m (OH), 3146 w (NH), 1673 m (C=O), 1621 w (HOH), 1600 m (C=O), 1032 br (S=O, dmsO), 694 m, 673 sh (Al–F).

$[GaF_3(L^1)]$. A solution of $[GaF_3(dmsO)(OH_2)_2]$ (0.034 g, 0.142 mmol) in MeOH (5 mL) was added to a solution of L^1 (0.075 g, 0.142 mmol) in MeOH (5 mL). This was left to stir at room temperature for 4 h, then heated at 60 °C for 2 h. The solvent was then removed *in vacuo*, and the product was isolated as an off-white solid. Yield: 0.060 g, 0.091 mmol (64%). Anal. required for $C_{30}H_{36}F_3GaN_6O_3 \cdot dmsO \cdot H_2O$: C, 51.14; H, 5.90; N, 11.18. Found: C, 51.43; H, 5.95; N, 11.58%. 1H NMR (298 K, CD_3OD): δ (ppm) = 7.62–7.53 (br m, [6H], ArH), 7.38–7.29 (br m, [6H], ArH), 7.18 (br s, [NH]), 7.10–7.08 (m, [3H], ArH), 4.85 (s, H₂O), 4.05 (s, [6H], CH₂), 3.45 (br s, [12H], tacn-CH₂), 2.66 (s, dmsO). $^{13}C\{^1H\}$ NMR (CD_3OD , 298 K): δ (ppm) = 168.3 (C=O), 139.6 (ArC), 130.0 (ArC), 125.5 (ArC), 121.4 (ArC), 58.5 (CH₂), 50.2 (tacn-CH₂), 40.6 (dmsO). $^{19}F\{^1H\}$ NMR (CD_3OD , 298 K): δ (ppm) = –180 (v br with partially resolved coupling to ^{69/71}Ga). ^{71}Ga NMR (CD_3OD , 298 K): δ (ppm) = 46.6 (br quartet, ¹J_{Ga-¹⁹F} ~ 510 Hz). ESI⁺ MS (CH₃OH): found: 635.4 (expected for $[GaF_2(L^1)]^+$: m/z = 635.2). IR (Nujol, ν/cm^{-1}): 3425 br (OH), 3195 w, 3133 w (NH), 1685 s (C=O), 1621 sh (HOH), 1599 s (C=O), 1015 m (S=O, dmsO), 583, 543 w (Ga–F). Crystals suitable for X-ray diffraction were grown *via* vapour diffusion of diethyl ether into a methanol solution of the product.

$[FeF_3(L^1)]$. A suspension of $FeF_3 \cdot 3H_2O$ (0.016 g, 0.095 mmol) in EtOH (7.5 mL) was added to a solution of L^1 (0.050 g, 0.095 mmol) in EtOH (7.5 mL). The reaction mixture was stirred at reflux for four hours, giving a pale-yellow solution. The solvent volume was then reduced to approx. 2 mL *in vacuo* and diethyl ether (20 mL) was added, causing precipitation of an off-white solid. This was filtered and dried *in vacuo*. Yield: 0.041 g, 0.064 mmol (67%). Anal. required for $C_{30}H_{36}F_3FeN_6O_3 \cdot H_2O \cdot 0.25EtOH$: C, 54.81; H, 6.08; N, 12.22. Found: C, 54.55; H, 6.05; N, 12.31%. IR (Nujol, ν/cm^{-1}): 3400 br, 3300 br (OH), 3197 m, 3136 w (NH), 1681 s, 1599 s (C=O), 550, 537 w (Fe–F). ESI⁺ MS (MeOH): not observed.

$[AlF_3(L^2)]$. A solution of $[AlF_3(dmsO)(OH_2)_2]$ (0.011 g, 0.054 mmol) in MeOH (5 mL) was added to a solution of L^2 (0.025 g, 0.054 mmol) in MeOH (5 mL). The mixture was stirred overnight at room temperature. The solvent was removed *in vacuo* to leave a sticky hygroscopic solid. This was



washed with diethyl ether (3 × 10 mL) and dried *in vacuo*, leaving a white powdered solid. Yield: 0.022 g, 0.040 mmol (74%). Anal. required for C₂₄H₄₈AlF₃N₆O₃·3H₂O: C, 45.36; H, 8.56; N, 13.22. Found: C, 45.19; H, 8.71; N, 13.11%. ¹H NMR (CD₃OD, 298 K): δ (ppm) = 4.85 (H₂O), 3.96 (septet, ³J_{H-H} = 6.6 Hz, [3H], ¹Pr-CH), 3.18–3.13 (m, [6H], CH₂), 2.85–3.03 (br m, [12H], tacn-CH₂), 2.66 (s, dmsO), 2.51–2.48 (m, [6H], CH₂), 1.14 (d, ³J_{H-H} = 6.6 Hz, [18H], ¹Pr-CH₃). ¹H NMR (D₂O, 298 K): δ (ppm) = 3.93–3.83 (br septet, [3H], ¹Pr-CH), 3.15–3.11 (br t, [6H], CH₂), 2.89 (br s, [12H], tacn-CH₂), 2.51–2.48 (br t, [6H], CH₂), 1.11 (br d, [18H], ¹Pr-CH₃). ¹³C{¹H} NMR (CD₃OD, 298 K): δ (ppm) = 172.7 (C=O), 53.1 (CH₂), 51.2 (tacn-CH₂), 42.7 (¹Pr-CH), 33.4 (CH₂), 22.8 (¹Pr-CH₃). ¹³C{¹H} NMR (D₂O, 298 K): δ (ppm) = 172.4 (C=O), 50.9 (CH₂), 48.6 (tacn-CH₂), 41.8 (¹Pr-CH), 32.1 (CH₂), 21.4 (¹Pr-CH₃). ¹⁹F{¹H} NMR (CD₃OD, 298 K): δ (ppm) = –196 (br); (D₂O, 298 K): δ (ppm) = –155 (br). ²⁹Al NMR (CD₃OD, 298 K): not observed. HR ESI⁺ MS (CH₃OH): found: 553.3627 (expected for [AlF₃(L²) + H]⁺: m/z = 553.3628), 491.3681 (expected for [L² + Na]⁺: m/z = 491.3680), 469.3876 (expected for [L² + H]⁺: m/z = 469.3861). IR (Nujol, ν/cm⁻¹): 3430 v br, 3290 br (OH), 3090 br, 3068 br (NH), 1644 s, 1551 s (C=O), 1050 w (S=O, dmsO), 667 br, 616 sh (Al-F).

[GaF₃(L²)]. A solution of [GaF₃(dmsO)(OH₂)₂] (0.032 g, 0.134 mmol) in MeOH (5 mL) was added to a solution of L² (0.063 g, 0.134 mmol) in MeOH (5 mL). The mixture was stirred at room temperature for 48 h and then concentrated to ca. 2 mL *in vacuo*. Diethyl ether (20 mL) was added, causing a pale-yellow precipitate to form. This was collected by filtration as a very hygroscopic, sticky solid, which became an off-white powder upon drying *in vacuo*. Yield: 0.067 g, 0.112 mmol (84%). Anal. required for C₂₄H₄₈F₃GaN₆O₃·3H₂O·0.3dmsO: C, 44.00; H, 7.93; N, 12.70. Found: C, 43.91; H, 8.36; N, 12.49%. ¹H NMR (CD₃OD, 298 K): δ (ppm) = 4.85 (H₂O), 3.93 (septet, ³J_{H-H} = 6.4 Hz [3H], ¹Pr-CH), 3.42–3.38 (br m, [6H], CH₂), 3.16–3.06 (br m, [6H], tacn-CH₂), 3.82–3.76 (br m, [6H], tacn-CH₂), 2.66 (dmsO), 2.53–2.47 (br m, [6H], CH₂), 1.13 (d, ³J_{H-H} = 6.4 Hz, [18H], ¹Pr-CH₃). ¹³C{¹H} NMR (CD₃OD, 298 K): δ (ppm) = 172.6 (C=O), 54.6 (¹Pr-CH), 53.1 (CH₂), 51.2 (tacn-CH₂), 42.7 (tacn-CH₂), 40.6 (dmsO), 33.4 (CH₂), 22.8 (¹Pr-CH₃). ¹⁹F{¹H} NMR (CD₃OD, 298 K): δ (ppm) = –178.2 (br). ⁷¹Ga NMR (CD₃OD, 298 K): δ (ppm) = 41.0 (br quartet, ¹J_{Ga-¹⁹F} ~ 520 Hz). ESI⁺ MS (CH₃OH): found: 575.5 (expected for [GaF₂(L²)⁺: m/z = 575.3). IR (Nujol, ν/cm⁻¹): 3438 br, 3267 br (OH), 3190 sh, 3060 br (NH), 1645 br s, 1548 s (C=O), 1018 w (S=O, dmsO), 528 m, 510 sh (Ga-F).

Attempted preparation of [InF₃(L²)]. A solution of [InF₃(dmsO)(OH₂)₂] (0.037 g, 0.128 mmol) in MeOH (5 mL) was added to a solution of L² (0.060 g, 0.128 mmol) in MeOH (5 mL). The mixture was refluxed with stirring for 2 h. The solution was concentrated to ca. 2 mL *in vacuo*, and diethyl ether (20 mL) was added, causing precipitation of an off-white solid. This was isolated *via* filtration as a very hygroscopic, sticky solid. Upon further drying *in vacuo*, a white powder product was obtained. Yield: 0.026 g. ¹H NMR spectroscopy indicates that the isolated product appears to contain two different indium species, one of which is the target complex,

while the second is as yet unidentified; a significant amount of F⁻ is also present (¹⁹F NMR evidence). Spectroscopic data quoted here are those tentatively assigned to the target [InF₃(L²) complex. ¹H NMR (CD₃OD, 298 K): δ (ppm) = 4.85 (H₂O), 3.96 (br septet, [3H], ¹Pr-CH), 3.15 (br t, CH₂), 3.12–3.02 (br m, [6H], tacn-CH₂), 2.99–2.88 (br m, [6H], tacn-CH₂), 2.74–2.69 (br m, [2H], CH₂), 2.66 (dmsO), 2.65–2.61 (m, [2H], CH₂), 2.52–2.45 (br m, [2H], CH₂), 1.14 (br d, [18H], ¹Pr-CH₃). ¹⁹F{¹H} NMR (CD₃OD, 298 K): δ (ppm) = –197.8 (br) (a singlet is also observed at –132.6 ppm, suggesting significant liberation of F⁻ from the indium(III) during the reaction, along with a minor species giving a broad resonance at –202 ppm). A few small crystals of [InF₃(L²) were grown *via* slow evaporation from the NMR solution of the product mixture in d₄-methanol and were analysed by single crystal X-ray diffraction.

[FeF₃(L²)]. A suspension of FeF₃·3H₂O (0.019 g, 0.112 mmol) in EtOH (7.5 mL) was added to a solution of L² (0.053 g, 0.112 mmol) in EtOH (7.5 mL). The solution was heated to 80 °C, at which point the solution changed from colourless to orange-yellow and full dissolution was observed. Heating was continued for 4 h, then the solvent was removed *in vacuo*. An off-white solid remained. Yield: 0.036 g, 0.068 mmol (61%). Anal. required for C₂₄H₄₈FeF₃N₆O₃·3H₂O: C, 45.36; H, 8.56; N, 13.22. Found: C, 45.73; H, 8.19; N, 13.11%. IR (Nujol, ν/cm⁻¹): 3450 s br, 3275 s br (OH), 3091 sh, 3075 m br (NH), 1648 s, 1555 s (C=O), 512 (br, Fe-F). HR ESI⁺ MS (CH₃OH): found: m/z = 562.3110 [FeF₂(L²)⁺ (calculated: m/z = 562.3105), 449.2263 [FeF₂(¹PrC(O)NH(CH₂)₂)₂-tacn + H]⁺ (calculated: m/z = 449.2265), 262.1578 [Fe(L²)²⁺ (calculated: m/z = 262.1563).

[AlF₃(L³)]. A solution of [AlF₃(dmsO)(OH₂)₂] (0.026 g, 0.130 mmol) in MeOH (5 mL) was added to a solution of L³ (0.45 g, 0.130 mmol) in MeOH (5 mL). This was left to stir at room temperature overnight. The solvent was then concentrated *in vacuo* to ca. 2 mL, then diethyl ether (10 mL) was added, causing the precipitation of a white solid, which was collected by filtration and dried *in vacuo*. Yield: 0.038 g, 0.087 mmol (67%). Anal. required for C₂₀H₃₄AlF₃N₄O·2H₂O·dmsO: required: C, 48.16; H, 7.77; N, 10.70. Found: C, 48.52; H, 8.14; N, 10.29%. ¹H NMR (CD₃OD, 298 K): δ (ppm) = 7.60–7.52 (m, [2H], ArH), 7.33–7.28 (m, [2H], ArH), 7.10–7.06 (m, [1H], ArH), 4.86 (H₂O), 3.59 (s, [2H], CH₂), 3.35 (br septet, overlapping with solvent peaks, ¹Pr-CH), 3.15–3.02 (br m, [4H], tacn-CH₂), 2.97–2.80 (br m, [8H], tacn-CH₂), 2.66 (dmsO), 1.29 (d, ³J_{H-H} = 6.5 Hz, [6H], ¹Pr-CH₃), 1.23 (d, ³J_{H-H} = 6.6 Hz, [6H], ¹Pr-CH₃). ¹³C{¹H} NMR (298 K, CD₃OD): δ (ppm) = 164.6 (C=O), 140.0 (ArC), 130.0 (ArC), 125.3 (ArC), 121.1 (ArC), 58.6 (CH₂), 55.3 (¹Pr-CH), 50.3 (tacn-CH₂), 48.3 (tacn-CH₂), 46.3 (tacn-CH₂), 18.5, 18.1 (¹Pr-CH₃). ¹⁹F{¹H} NMR (CD₃OD, 298 K): δ (ppm) = –196 (br); (D₂O, 298 K): δ (ppm) = –155.2 ([1F], –156.1 ([2F]). ²⁷Al NMR (CD₃OD, 298 K): not observed. ESI MS⁺ (CH₃OH) found: m/z = 431.2570 (expected for [AlF₃(L³) + H]⁺: m/z = 431.2573), 347.2817 (expected for [L³ + H]⁺: m/z = 347.2805), 174.1441 (expected for [L³ + 2H]²⁺: m/z = 174.1439). IR (Nujol, ν/cm⁻¹): 3430 (br, OH), 3266, 3177 (NH), 3155 (aromatic CH), 2727, 2676 (C-H stretch), 1693, 1615, 1600 (C=O), 642, 592 sh (Al-F).



[GaF₃(L³)]. A solution of [GaF₃(dmsO)(OH₂)₂] (0.038 g, 0.159 mmol) in MeOH (5 mL) was added to a solution of L³ (0.55 g, 0.159 mmol) in MeOH (5 mL). This was left to stir at room temperature overnight. The solvent was concentrated *in vacuo* to ca. 2 mL, then diethyl ether (10 mL) was added, causing the precipitation of a white solid. The solid was collected by filtration and dried *in vacuo*. Yield: 0.046 g, 0.097 mmol (61%). Anal. required for C₂₀H₃₄F₃GaN₄O·3H₂O: required: C, 45.56; H, 7.65; N, 10.63. Found: C, 45.74; H, 7.28; N, 10.25%. ¹H NMR (CD₃OD, 298 K): δ (ppm) = 7.60–7.55 (m, [2H], ArH), 7.32–7.27 (m, [2H], ArH), 7.11–7.05 (m, [1H], ArH), 4.86 (H₂O), 3.60 (s, [2H], CH₂), 3.35 (septet, ³J_{H-H} = 6.9 Hz, [2H], ¹Pr-CH), 3.14–3.01 (m, [4H], tacn-CH₂), 2.99–2.79 (br m, [8H], tacn-CH₂), 2.66 (dmsO), 1.29 (d, ³J_{H-H} = 6.6 Hz, [6H], ¹Pr-CH₃), 1.23 (d, ³J_{H-H} = 6.6 Hz, [6H], ¹Pr-CH₃). ¹³C{¹H} NMR (298 K, CD₃OD): δ (ppm) = 171.4 (C=O), 140.0 (ArC), 130.0 (ArC), 125.5 (ArC), 121.1 (ArC), 58.7 (CH₂), 55.3 (¹Pr-CH), 50.3 (tacn-CH₂), 48.3 (tacn-CH₂), 46.3 (tacn-CH₂), 40.6 (dmsO), 18.5, 18.1 (¹Pr-CH₃). ¹⁹F{¹H} NMR (CD₃OD, 298 K): δ (ppm) = –171.5 (br s, [2F]) –172.3 (br s, [1F]). ⁷¹Ga NMR (298 K, MeOH): not observed. ESI⁺ MS (CH₃OH): found: *m/z* = 473.3429 (expected for [GaF₃(L³) + H]⁺: *m/z* = 473.2019); 453.1950 (expected for [GaF₂(L³)⁺: *m/z* = 453.1956), 347.2817 (expected for [L³ + H]⁺: *m/z* = 347.2805), 305.2331 (expected for [L³-¹Pr][H]⁺: *m/z* = 305.2336). IR (Nujol, ν/cm⁻¹): 3420, 3307 (OH), 3193, 3132 (NH), 1689, 1622 (C=O), 1032 (S=O, dmsO), 539, 520 (GaF). Crystals suitable for X-ray structure determination were grown *via* slow evaporation from a solution of the complex in acetonitrile.

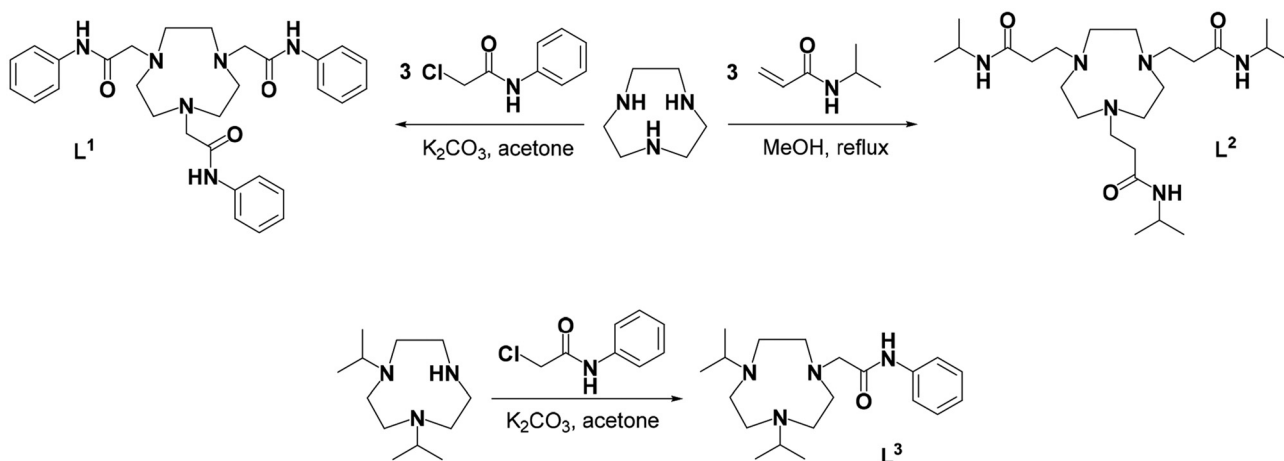
[FeF₃(L³)]. A suspension of FeF₃·3H₂O (0.020 g, 0.117 mmol) in EtOH (7.5 mL) was added to a solution of L³ (0.041 g, 0.117 mmol) in EtOH (7.5 mL). This was stirred at reflux. After 30 min full dissolution was observed and refluxing was continued for 6 h. The solvent was removed *in vacuo*. An off-white solid remained. Yield: 0.034 g, 0.074 mmol (63%). Anal. required for C₂₀H₃₄F₃FeN₄O·1.5H₂O: required: C, 49.39; H, 7.67; N, 11.52. Found: C, 49.76; H, 7.84; N, 11.16%. IR (Nujol, ν/cm⁻¹): 3428, 3270 (OH), 3206 sh, 3192(NH), 1689 (C=O),

1617 sh (HOH), 1598 (C=O), 539, 521 (FeF). HR ESI⁺ MS (CH₃OH): found: *m/z* = 440.2043 [FeF₂(L³)⁺ (calculated: *m/z* = 440.2050), 347.2809 (expected for [L³ + H]⁺: *m/z* = 347.2805). Crystals suitable for X-ray diffraction were grown *via* slow evaporation from a solution of the product in methanol/diethyl ether.

Results and discussion

The target amide-functionalised tacn ligands, L¹–L³ were selected to explore the effects of (i) varying the linker between the amine and amide groups (*i.e.* L¹ vs. L²) and (ii) the number of amide groups present (*i.e.* L¹ vs. L³). The phenyl groups present in L¹ and L³ also provide a convenient chromophore to track the complexes in subsequent radiochemistry experiments. L¹–L³ were prepared as shown in Scheme 2, *via* reaction of tacn with K₂CO₃ and three mol. equiv. of 2-chloro-*N*-phenylacetamide in acetone at room temperature (18 h) (L¹), *N*-isopropylacrylamide in refluxing MeOH (L²), or by reaction of preformed ¹Pr₂-tacn with one mol. equiv. of 2-chloro-*N*-phenylacetamide and K₂CO₃ in acetone. Following work-up and flash chromatography (L¹ and L³), the pure ligands were isolated as a white powder (L¹), yellow oil (L²) or orange oil (L³) and characterised by ¹H and ¹³C{¹H} NMR and IR spectroscopy, UV-HPLC analysis (L¹ and L³) and *via* high resolution ESI⁺ MS. The IR spectra show two strong C=O stretching vibrations for each of L¹–L³, along with the expected ν(NH) bands.

To further confirm the identity of L¹, a small sample was converted to its protonated form by addition of HCl_{aq} to a solution of L¹ in MeOH and crystallised from *via* slow evaporation over a few weeks. The structure of L¹·HCl was then determined by X-ray crystallography, which confirmed the presence of the *tris*-amide tacn moiety (L¹) and showed (Fig. 1) mono-protonation of the tacn ring. *Intramolecular* N6–H6···O1(=C) H-bonding between the amide groups is evident between two of the pendant arms of L¹·HCl, while *intermolecular*



Scheme 2 Routes for preparation of ligands L¹–L³.



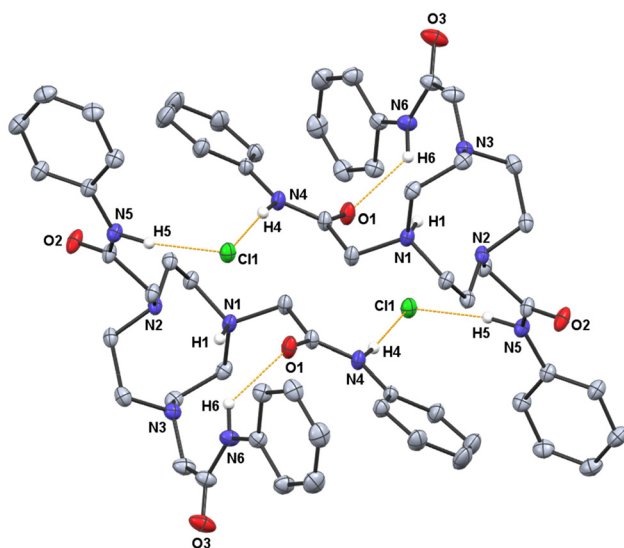


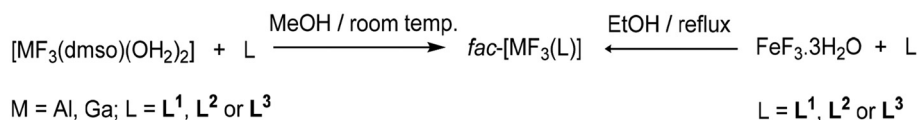
Fig. 1 View of the structure of $L^1 \cdot HCl$ showing the weakly H-bonded centrosymmetric dimer present, with the $N-H \cdots Cl \cdots H-N$ hydrogen bonding interactions marked with dashed lines and the atom numbering scheme shown. H atoms are omitted for clarity (except for those bonded to the N atoms). Ellipsoids are drawn at the 50% probability level.

H-bonding involving the chloride anion and involving the third amide arm in two adjacent L^1 moieties, $C(O)N4-H4 \cdots Cl1 \cdots H5-N5C(O)$ gives rise to weakly associated dimers in the solid state ($N4H4 \cdots Cl = 2.130$, $N5H5 \cdots Cl = 2.166 \text{ \AA}$).

A few crystals of $L^1 \cdot HNO_3$ were also isolated as a minor by-product during this study, from an attempt to react L^1 with $Ga(NO_3)_3 \cdot 9H_2O$ in MeOH; the structure of this salt is shown in ESI Fig. S16.†

Reactions of L^1-L^3 with $[MF_3(dmsO)(OH_2)_2]$ ($M = Al, Ga, In$) and $FeF_3 \cdot 3H_2O$

While the poorly soluble (and usually polymeric)²⁸ $MF_3 \cdot 3H_2O$ ($M = Al, Ga, In$) precursors can provide a source of MF_3 for coordination to certain ligands under high temperature and pressure (solvothetical) conditions,^{4,30} we have shown previously that the molecular $[MF_3(dmsO)(OH_2)_2]$ are often more suitable precursors due their higher solubilities under milder reaction conditions, and therefore better compatibility with a wider range of ligand types and functionalities.^{29,30} Since the pendant amide functions may be susceptible to hydrolysis, the $[MF_3(dmsO)(OH_2)_2]$ complexes were chosen as the metal trifluoride precursors for the present study to facilitate the coordination chemistry under milder reaction conditions, as illustrated in Scheme 3. Treatment of $[MF_3(dmsO)(OH_2)_2]$ ($M =$



Scheme 3 Synthesis methods for the complexes, $fac-[MF_3(L)]$ ($M = Al, Ga, Fe; L = L^1-L^3$).

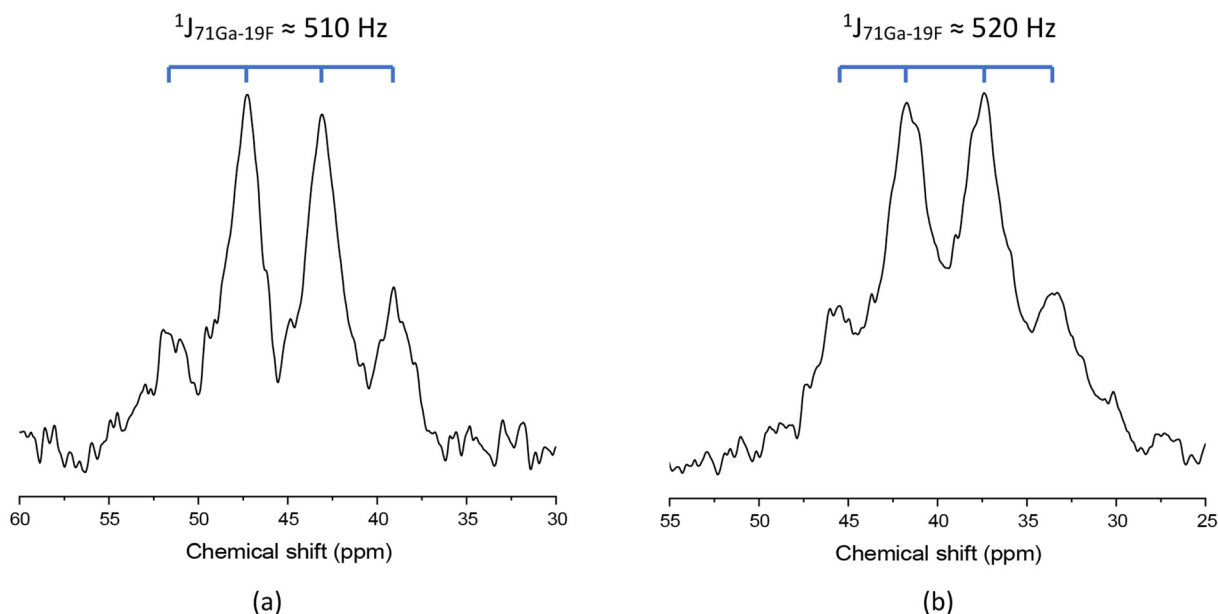


Fig. 2 ^{71}Ga NMR spectra of (a) $[GaF_3(L^1)]$ and (b) $[GaF_3(L^2)]$, each showing the expected broad 1 : 3 : 3 : 1 quartet $^1J_{^{71}Ga^{19}F}$ coupling (CD_3OD).



Al, Ga) with one mol. eq. of L ($L = L^1-L^3$) at room temperature or with gentle heating (60 °C, $M = Ga$) affords the distorted octahedral complexes *fac*-[MF₃(L)] as white powdered solids and their spectroscopic and structural data are discussed below. For $M = Al$, short reaction times (2–6 h at room temperature) gave higher yields of the target complexes, while refluxing in MeOH overnight led to precipitation of some white solid that needed to be separated before the target complexes were isolated from the filtrate. The isolated yields for the Al(III) and Ga(III) complexes were typically in the range 65–80%. However, for In(III), despite several attempts and varying the reaction conditions, the reaction of [InF₃(dmsO)(OH₂)₂] with L¹ repeatedly gave a mixture of products and a

pure sample of [InF₃(L¹)] could not be isolated. Also, in the case of the [InF₃(dmsO)(OH₂)₂]/L² reaction, elemental analysis on samples from different batches did not match the expected values, and while ¹H and ¹⁹F{¹H} NMR spectroscopic analysis indicated the presence of [InF₃(L²)] (which was also confirmed by a single crystal X-ray structure analysis – discussed below), a second, unidentified product, along with a significant amount of free F⁻ were also present. The production of a mixture of species may be a consequence of the weaker M–F bonds present in the In(III) species (compared to Al(III) and Ga(III)), resulting in competition for coordination to In(III) of one or more amide pendant groups and loss of F⁻. However, given these results, the indium chemistry was not pursued further.

In the case of the Fe(III) complexes, the precursor, FeF₃·3H₂O, was reacted directly with L¹–L³, in EtOH solution at reflux. The three [FeF₃(L)] complexes were isolated in good yields as pale-yellow solids. While the expected $\nu(\text{Fe-F})$ bands are present in the IR spectra and the expected peaks are evident in the ESI⁺ MS for [FeF₃(L²)], the paramagnetic nature of these complexes precludes any useful NMR analysis.

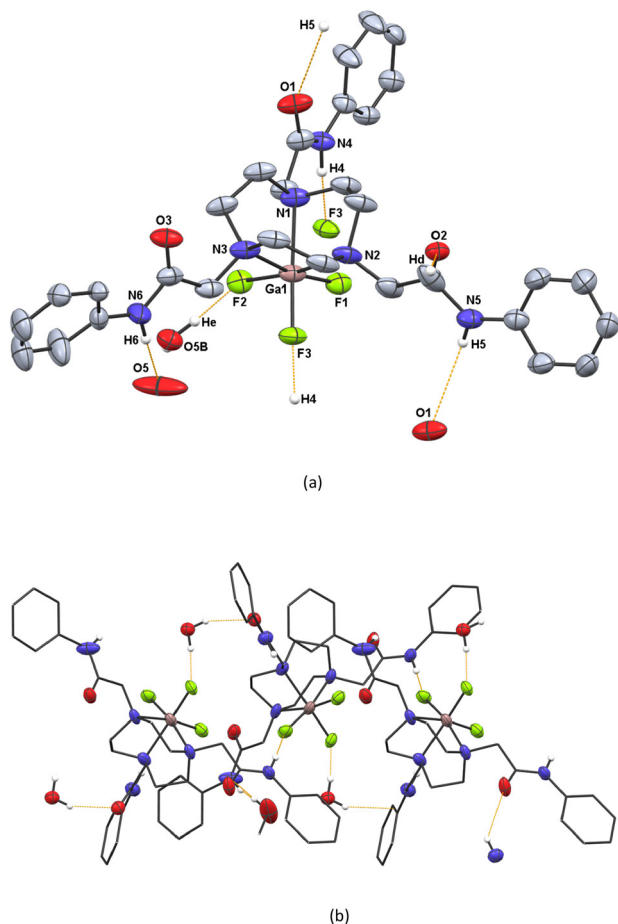


Fig. 3 (a) View of the structure of the component of [GaF₃(L¹)]·MeOH·0.5H₂O with the H-bonding, showing the atom numbering scheme. H atoms (except amide N–H and lattice H₂O) and lattice MeOH molecules are omitted for clarity (note that there is disorder in two of the pendant arms – see ESI). Ellipsoids are drawn at the 50% probability level. Selected bond lengths (Å) and angles (°): Ga1–F1 = 1.8287(18), Ga1–F2 = 1.8487(17), Ga1–F3 = 1.8493(16), Ga1–N1 = 2.157(2), Ga1–N2 = 2.162(2), Ga1–N3 = 2.165(3), F2–Ga1–F1 = 96.23(8), F3–Ga1–F1 = 96.31(8), F3–Ga1–F2 = 96.23(8), N2–Ga1–N1 = 82.80(9), N3–Ga1–N1 = 82.30(9), N3–Ga1–N2 = 81.86(11); (b) view of part of the H-bonded extended structure showing the 1D chain formed via intermolecular F...H–N interactions (marked): contacts (F2...H4N4 = 1.758 Å, F3...H₂O = 1.695 Å).

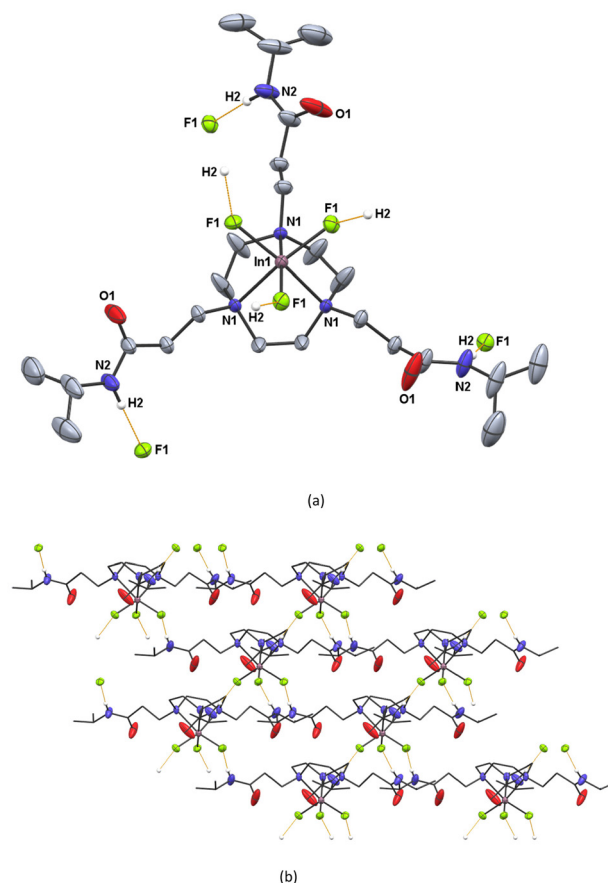


Fig. 4 (a) View of the structure of [InF₃(L²)] showing the atom numbering scheme. H atoms are omitted for clarity. Ellipsoids on In, F, N and O are drawn at the 50% probability level. Selected bond lengths (Å) and angles (°): In1–F1 2.071(2), In1–N1 2.299(3), F1–In1–F1 = 97.99(8), N1–In1–N1 = 78.04(10); (b) view down the *a*-axis showing the intermolecular F...HN hydrogen bonding contacts.



The powdered $[\text{MF}_3(\text{L})]$ products show either two ($a_1 + e$) or one broad M–F stretching vibration in the far IR regions as expected, and the observed frequencies compare well with the literature data for $[\text{MF}_3(\text{Me}_3\text{-tacn})]$ ($\text{M} = \text{Al}, \text{Ge}, \text{Fe}$).^{4,13} The IR spectra also confirm the presence of H_2O and in some cases dmsO in the isolated products. This was also consistent with microanalytical data, while ESI-MS typically showed peaks with the expected isotopic pattern associated with $[\text{MF}_2(\text{L})]^+$ or in some cases $[\text{MF}_3(\text{L}) + \text{H}]^+$, as expected, although often with low intensities; peaks for $[\text{L} + \text{H}]^+$ are also observed in a number of cases.

Solution multinuclear NMR studies were hindered somewhat by the limited solubilities of the new complexes, especially in non-protic solvents. Hence spectra were mostly obtained from H_2O or MeOH solutions. For the GaF_3 complexes involving L^1 and L^2 the *fac*-octahedral geometry is unambiguously assigned from the ^{71}Ga and $^{19}\text{F}\{^1\text{H}\}$ NMR spectra. Thus, the ^{71}Ga spectra each show a broadened 1:3:3:1 quartet in the range +40 to +50 ppm, arising from coupling of the quadrupolar ^{71}Ga nucleus to the three *facial* fluorides, $^1J_{^{71}\text{Ga}-^{19}\text{F}} \sim 510\text{--}520$ Hz (Fig. 2), and a very broad resonance for each complex in the $^{19}\text{F}\{^1\text{H}\}$ NMR spectra at ~ -180 ppm, caused by two overlapping, partially resolved 1:1:1:1 quartets due to coupling of the ^{19}F to both the ^{69}Ga and ^{71}Ga nuclei (each of which has $I = 3/2$), respectively, in the approximately C_{3v} symmetry molecules. These chemical shifts and couplings are comparable with those reported for $[\text{GaF}_3(\text{Me}_3\text{-tacn})]$ and $[\text{GaF}_3(\text{BnMe}_2\text{-tacn})]$.⁴

Two ^{19}F NMR resonances are expected for the lower symmetry $[\text{MF}_3(\text{L}^3)]$ complexes, these are observed at -155.2 ([1F]), -156.1 ([2F]) for $\text{M} = \text{Al}$ (D_2O), and at -171.5 ([2F]) and -172.3 ppm ([1F]) for $\text{M} = \text{Ga}$ (MeOH), although the F–F couplings are lost in the line widths. No ^{71}Ga NMR resonance was observed for $[\text{GaF}_3(\text{L}^3)]$, probably because of the lower symmetry arising from the asymmetrically substituted tacn N-donor atoms. The ^1H and $^{13}\text{C}\{^1\text{H}\}$ NMR spectra for $[\text{MF}_3(\text{L}^3)]$ ($\text{M} = \text{Al}, \text{Ga}$) also show that the two CH_3 groups in the ^1Pr pendant groups become diastereotopic in the complexes, as expected, providing further supporting evidence for the successful complexation of the MF_3 fragments to L^3 .³¹

The ^{19}F NMR shifts for the complexes show a significant solvent dependence in MeOH and H_2O . This is attributed to the highly polar nature of the pyramidal MF_3 units present and their strong tendency to hydrogen bond to adjacent H-bond donors, including both the pendant amide groups and protic solvent molecules (as is also observed in the crystal structures – below).

Further confirmation of the molecular structures and the nature and extent of hydrogen-bonding present in $[\text{GaF}_3(\text{L}^1)] \cdot 1.5\text{MeOH} \cdot 0.5\text{H}_2\text{O}$, $[\text{InF}_3(\text{L}^2)]$, $[\text{GaF}_3(\text{L}^3)]$ and $[\text{FeF}_3(\text{L}^3)]$ were obtained by single crystal X-ray analyses.

The structure of $[\text{GaF}_3(\text{L}^1)] \cdot 1.5\text{MeOH} \cdot 0.5\text{H}_2\text{O}$ (Fig. 3) shows the Ga(III) atom in a distorted octahedral coordination environment, with the tridentate tacn ring occupying one face of the Ga ($\text{Ga}-\text{N}1 = 2.157(2)$, $\text{Ga}-\text{N}2 = 2.162(2)$, $\text{Ga}-\text{N}3 = 2.165(3)$ Å),

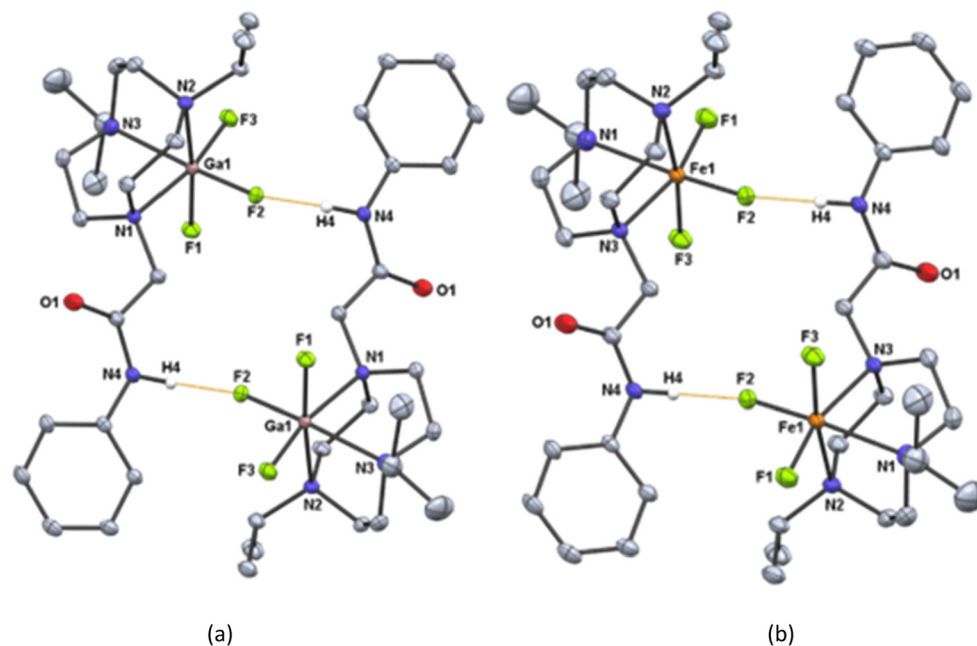


Fig. 5 View of the isostructural metal complexes present in (a) $[\text{GaF}_3(\text{L}^3)]$ and (b) $[\text{FeF}_3(\text{L}^3)]$, showing the atom numbering schemes and the intermolecular 'head-to-tail' $\text{F}2 \times \text{H}4-\text{N}4$ hydrogen bonding interactions, giving weakly associated dimers. H atoms and lattice solvent are omitted for clarity. Ellipsoids are drawn at the 50% probability level. Selected bond lengths (Å) and angles ($^\circ$): $[\text{GaF}_3(\text{L}^3)] \times 0.067\text{H}_2\text{O}$: $\text{Ga}-\text{F}1 = 1.8392(3)$, $\text{Ga}-\text{F}2 = 1.8613(3)$, $\text{Ga}-\text{F}3 = 1.824(3)$, $\text{Ga}-\text{N}1 = 2.1674(4)$, $\text{Ga}-\text{N}2 = 2.2007(4)$, $\text{Ga}-\text{N}3 = 2.2057(4)$, $\text{F}2-\text{Ga}-\text{F}1 = 93.541(13)$, $\text{F}3-\text{Ga}-\text{F}1 = 95.564(12)$, $\text{F}3-\text{Ga}-\text{F}2 = 98.067(12)$, $\text{N}3-\text{Ga}-\text{N}2 = 82.448(15)$, $\text{N}1-\text{Ga}-\text{N}2 = 82.582(14)$, $\text{N}1-\text{Ga}-\text{N}3 = 81.818(15)$; $[\text{FeF}_3(\text{L}^3)] \cdot 0.083\text{MeOH}$: $\text{Fe}1-\text{F}1 = 1.8446(7)$, $\text{Fe}1-\text{F}2 = 1.8824(7)$, $\text{Fe}1-\text{F}3 = 1.8605(7)$, $\text{Fe}1-\text{N}1 = 2.2643(10)$, $\text{Fe}1-\text{N}2 = 2.2668(10)$, $\text{Fe}1-\text{N}3 = 2.2328(9)$, $\text{F}1-\text{Fe}1-\text{F}2 = 101.01(3)$, $\text{F}1-\text{Fe}1-\text{F}3 = 97.95(3)$, $\text{F}3-\text{Fe}1-\text{F}2 = 94.91(3)$, $\text{N}1-\text{Fe}1-\text{N}2 = 80.04(4)$, $\text{N}3-\text{Fe}1-\text{N}1 = 79.47(4)$, $\text{N}3-\text{Fe}1-\text{N}2 = 80.06(3)$.



and the three *facial* fluorides lying *trans* to the amine N-donor atoms, Ga–F1 = 1.8287(18), Ga–F2 = 1.8487(17), Ga–F3 = 1.8493(16) Å, in accord with the corresponding bond distances reported for [GaF₃(Me₃-tacn)]·4H₂O.⁴ The structure is disordered, with two distinct forms modelled (50 : 50 occupancy) displaying different orientations for one of the pendant amide arms (see Experimental). Hydrogen bonding is evident in one of the components between an amide N–H group or lattice water molecule and the F ligands in an adjacent molecule.

The reaction of [InF₃(dmsO)(H₂O)₂] with L¹–L³ under similar conditions to the Al(III) and Ga(III) complex syntheses produced a mixture of products. In one case we were able to obtain a few crystals of [InF₃(L²)] from the product mixture and confirmed its structure by single crystal X-ray analysis. [InF₃(L²)] crystallises in the trigonal space group R3c, with three-fold crystallographic symmetry. The structure (Fig. 4(a)) shows the distorted octahedral coordination at the metal ion *via* three *facial* fluorides and the three N-donor atoms from the tacn ring, *d*(In–F) = 2.071(2), *d*(In–N) = 2.299(3) Å. The F–In–F

angles are 97.99(8)°, while the N–In–N angles involving the macrocycle are much more acute (78.04(10)°). These values are in good accord with the corresponding metrics reported for [InF₃(Me₃-tacn)]·4H₂O and [InF₃(BnMe₂-tacn)]·1.2H₂O.⁴ Similarly to the case of [GaF₃(L¹)] discussed above, the pendant amide groups (in this case, –CH₂CH₂C(O)NHⁱPr, *i.e.* with the amide groups extended further from the macrocyclic amine functions by the extra CH₂ unit present in each pendant arm in L²) are not involved in coordination to indium(III), however, they each form one intermolecular N–H⋯F H-bond, *d*(N⋯F) = 1.888 Å, to an adjacent molecule, as illustrated in Fig. 4(b), to generate 2D sheets.

Crystals of both [GaF₃(L³)] (Fig. 5(a)) and [FeF₃(L³)] (Fig. 5(b)) were obtained as described in the Experimental section and are isostructural. Each complex shows *fac*-tridentate coordination of L³ to the metal ion *via* its tacn N(amine) donor atoms, with the three F[–] ligands occupying the other face and giving a distorted octahedral species. Both complexes form ‘head-to-tail’ H bonded dimers *via* hydrogen bonding

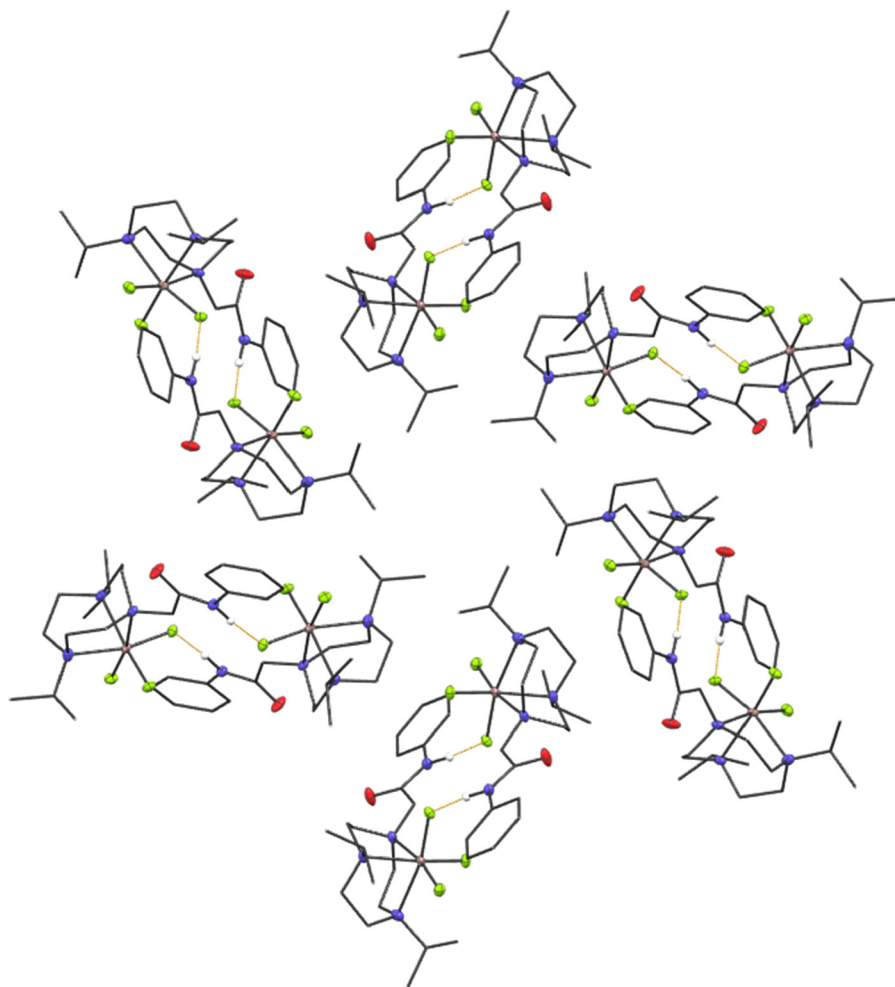


Fig. 6 View of the structure of [GaF₃(L³)] viewed down the *c*-axis showing the hexagonal arrangement adopted by the weakly associated dimers (the same arrangement is present in [FeF₃(L³)]).



Table 1 Summary of the results from $^{18}\text{F}/^{19}\text{F}$ isotopic exchange with $[\text{GaF}_3(\text{L}^1)]$ using a range of conditions

Precursor concentration ($\mu\text{mol mL}^{-1}$)	Temperature ($^{\circ}\text{C}$)	Time (min)	RCY (%)
1.5	80	10	7
1.5	80	10	6
3	80	10	20
3	80	10	19
3	80	10	18
3	80	10	15
3	80	20	15
3	80	30	17
3	60	10	9
3	60	20	13
3	60	30	16
3	RT	15	7
3	RT	30	10
3	RT	45	11
3	RT	60	14

Table 2 Summary of the results from SPE purification of $[\text{Ga}^{18}\text{FF}_2(\text{L}^1)]$ in $\text{H}_2\text{O}/\text{EtOH}$ and PBS/EtOH over 2 h

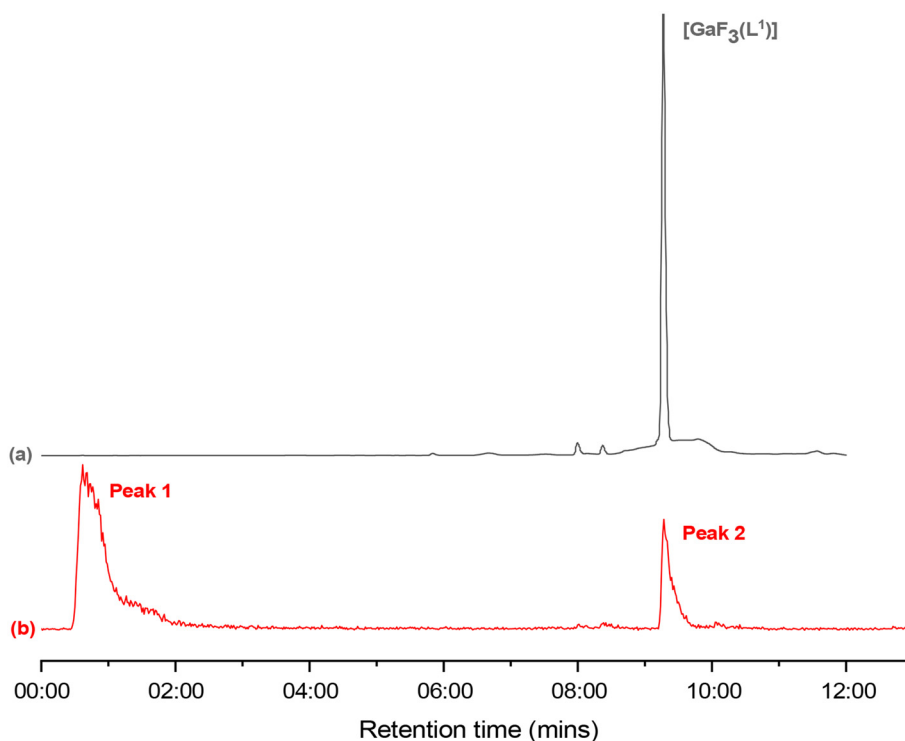
$[\text{Ga}^{18}\text{FF}_2(\text{L}^1)]$ in 90 : 10 $\text{H}_2\text{O} : \text{EtOH}$		$[\text{Ga}^{18}\text{FF}_2(\text{L}^1)]$ in 90 : 10 $\text{PBS} : \text{EtOH}$	
Time/min	RCP (%)	Time/min	RCP (%)
0	68	0	64
30	67	30	61
80	59	80	57
120	61	120	59

from the amide NH group is one molecule with one F atom in the second molecule ($M = \text{Fe} : \text{F} \cdots \text{HN}$ distance = 1.787 Å; $M = \text{Ga} : \text{F} \cdots \text{HN}$ distance = 1.769 Å).

Looking at the extended structures shows that the dimer units are arranged in a hexagonal 'windmill'-like array when viewed down the c -axis (Fig. 6). This leaves solvent accessible voids in the lattice containing disordered H_2O , which was modelled using a solvent mask, and consistent with *ca.* 1.20 and 2.40 H_2O molecules per unit cell for the Ga and Fe species, respectively. These complexes are also extremely hygroscopic, with the powders and crystals rapidly becoming sticky upon exposure to moist air over a few minutes.

Radiofluorination of $[\text{GaF}_3(\text{L}^1)]$ and $[\text{GaF}_3(\text{L}^3)]$

We have previously reported the radiofluorination of several gallium(III) macrocyclic complexes *via* both $\text{Cl}/^{18}\text{F}^4$ and $^{19}\text{F}/^{18}\text{F}^6$ exchange reactions in partially aqueous MeCN or EtOH solvent, including for the production of $[\text{Ga}^{18}\text{F}^{19}\text{F}_2(\text{BnMe}_2\text{-tactn})]$, which resulted in good radiochemical yields, and high radiochemical stability when formulated in EtOH with (aqueous) phosphate buffered saline at pH 7.4. We were therefore interested to explore the radiofluorination of both the $[\text{GaF}_3(\text{L}^1)]$ and $[\text{GaF}_3(\text{L}^3)]$ complexes by $^{18}\text{F}/^{19}\text{F}$ isotopic exchange to determine whether the presence of the strong H-bond donor pendant amide groups would affect the radiochemistry. Both of the precursor complexes also contain (at least) one Ph group, providing a chromophore for correlation of the UV trace of the precursor with the radioproduct(s).

**Fig. 7** (a) Analytical UV-HPLC trace of the reference standard compound $[\text{GaF}_3(\text{L}^1)]$, $R_t = 09 : 16$ min; (b) analytical radio-HPLC trace of the crude product from radiofluorination of $[\text{GaF}_3(\text{L}^1)]$. Peak 1: $R_t = 00 : 37$ min 80% ($^{18}\text{F}]\text{F}^-$). Peak 2: $R_t = 09 : 17$ min 20% ($[\text{Ga}^{18}\text{FF}_2(\text{L}^1)]$).

Radiofluorination experiments using $[\text{GaF}_3(\text{L}^1)]$ were performed by $^{18}\text{F}/^{19}\text{F}$ isotopic exchange in MeOH solution due to the poor solubility of the complex in other solvents such as MeCN and EtOH. While several different conditions were explored (Table 1), the highest RCY of *ca.* 20% was achieved reproducibly using 2 mg of the complex in MeOH, followed by the addition of $[\text{F}^{18}\text{F}]^-$ in target water (to give a $3.0 \mu\text{mol mL}^{-1}$ solution in 75% : 25% MeOH : H_2O) and heating this to 80 °C for 10 min (Table 2).

The radioproduct, $[\text{Ga}^{18}\text{FF}_2(\text{L}^1)]$, was identified by comparison of the *Rt* for the radiotracer and UV-HPLC trace of the radioproduct, and matching the latter with the UV-HPLC trace of the reference complex, $[\text{GaF}_3(\text{L}^1)]$ (Fig. 7). While using a lower precursor concentration ($1.5 \mu\text{mol mL}^{-1}$) also showed some radiofluorine incorporation, the RCY was lower (typically *ca.* 7%).

Purification was attempted using a solid phase extraction (SPE) cartridge method (see ESI†) before formulating the radioproduct in either 90 : 10 $\text{H}_2\text{O}/\text{EtOH}$ or 90 : 10 PBS/EtOH to investigate the radiochemical stability over a period of 2 h (Table 2). The RCP decreases by *ca.* 7% in $\text{EtOH}/\text{H}_2\text{O}$, and by *ca.* 5% in EtOH/PBS .

Several attempts to radiolabel solutions of $[\text{GaF}_3(\text{L}^3)]$ in MeOH, MeCN or EtOH using target water containing $[\text{F}^{18}\text{F}]^-$, either at room temperature for 30–60 min, or with heating (80 °C for 10–60 min), gave no evidence for radiofluorine uptake in any of these experiments.

Conclusions

This work has explored how tacn-based ligands incorporating one or more amide pendant functions coordinate to trivalent Group 13 metal trifluoride reagents, leading to three series of distorted octahedral complexes, *fac*- $[\text{MF}_3(\text{L})]$ for $\text{M} = \text{Al}, \text{Ga}$ and Fe ; $\text{L} = \text{L}^1\text{--L}^3$, in which the macrocycle coordinates *via* the three tacn amine donor groups only, leaving the amide functions (potential H-bond donors) uncoordinated, as confirmed by a combination of spectroscopic analyses and X-ray crystallographic studies on representative examples. In the solid state, significant intermolecular H-bonding involving the amide groups and one or more coordinated fluoride ligand is evident in all of the complexes producing an extended 3D polymer array for $[\text{InF}_3(\text{L}^2)]$. The L^3 complexes, $[\text{GaF}_3(\text{L}^3)]$ and $[\text{FeF}_3(\text{L}^3)]$ are isostructural and formed of ‘head-to-tail’ dimers that can be considered as inorganic analogues of the H-bonded dimers formed by amine thioureas with carboxylates that are observed frequently as ‘building blocks’ in supramolecular chemistry.

Radiofluorination experiments using $[\text{GaF}_3(\text{L}^1)]$ in aqueous MeOH and $[\text{F}^{18}\text{F}]^-$ in target water with brief heating (80 °C/10 min) showed modest uptake, giving a radiochemical yield (RCY) of ~20%, which was lower than observed previously for $[\text{GaF}_3(\text{BnMe}_2\text{-tacn})]$.⁶ Partial purification using a SPE protocol resulted in a RCP of 68% in $\text{H}_2\text{O}/\text{EtOH}$, and 64% in PBS/EtOH , however, both formulations showed some loss of $^{18}\text{F}^-$ over 2 h. Therefore, further efforts to remove unreacted $[\text{F}^{18}\text{F}]^-$ were not

pursued. The monoamide complex, $[\text{GaF}_3(\text{L}^3)]$, showed no clear evidence for $[\text{F}^{18}\text{F}]^-$ uptake under similar conditions.

Author contributions

Project conceptualisation and funding (GR, GMcR), ligand and complex synthesis (COC) and characterisation (COC, VKG, RPK, JMH), radiochemistry (COC, GMcR), data analysis, manuscript preparation and reviewing (all authors).

Data availability

The spectroscopic data for all of the new ligands and complexes are presented in the ESI† for this manuscript, along with X-ray crystallographic details and a table of crystallographic parameters, the radiolabelling methods and data. The cif files and checkcifs are available *via* the CCDC with reference numbers 2355936–2355941.† All of these data will also be publicly available *via* the University of Southampton’s permanent repository with a unique doi number.

Conflicts of interest

There are no conflicts to declare.

Acknowledgements

We thank the EPSRC for support through the Mithras Programme Grant (EP/SO32789/1) and through DTP grant number EP/T517859/1 (COG).

References

- 1 K. Chansaenpak, B. Vabre and F. P. Gabbaï, *Chem. Soc. Rev.*, 2016, **45**, 954.
- 2 W. Levason, F. M. Monzittu and G. Reid, *Coord. Chem. Rev.*, 2019, **391**, 90.
- 3 S. Schmitt and E. Moreau, *Coord. Chem. Rev.*, 2023, **480**, 215028.
- 4 R. Bhalla, C. Darby, W. Levason, S. K. Luthra, G. McRobbie, G. Reid, G. Sanderson and W. Zhang, *Chem. Sci.*, 2014, **5**, 381.
- 5 W. Levason, S. K. Luthra, G. McRobbie, F. M. Monzittu and G. Reid, *Dalton Trans.*, 2017, **46**, 14519.
- 6 F. M. Monzittu, I. Khan, W. Levason, S. K. Luthra, G. McRobbie and G. Reid, *Angew. Chem., Int. Ed.*, 2018, **57**, 6658.
- 7 M. S. Woodward, D. E. Runacres, J. Grigg, I. Khan, W. Levason, G. McRobbie and G. Reid, *Pure Appl. Chem.*, 2024, **96**, 57.
- 8 (a) P. Laverman, W. McBride, R. Sharkey, A. Eek, L. Joosten, W. Oyen, D. Goldenberg and O. Boerman, *J. Nucl. Med.*, 2010, **51**, 454; (b) W. McBride, C. D’Souza, R. Sharkey, H. Karacay, E. Rossi, C. Chang and D. Goldenberg,



- Bioconjugate Chem.*, 2010, **21**, 1331; (c) W. McBride, R. Sharkey, H. Karacay, C. D'Souza, E. Rossi, P. Laverman, C. Chang, O. Boerman and D. Goldenberg, *J. Nucl. Med.*, 2009, **50**, 991; (d) W. McBride, C. D'Souza, H. Karacay, R. Sharkey and D. Goldenberg, *Bioconjugate Chem.*, 2012, **23**, 538.
- 9 S. Schmitt and E. Moreau, *Coord. Chem. Rev.*, 2023, **480**, 215028.
- 10 R. Bhalla, W. Levason, S. K. Luthra, G. McRobbie, G. Sanderson and G. Reid, *Chem. – Eur. J.*, 2015, **21**, 4688.
- 11 J. N. Whetter, B. A. Vaughn, A. J. Koller and E. Boros, *Angew. Chem., Int. Ed.*, 2022, **61**, e202114203.
- 12 D. E. Runacres, V. K. Greenacre, J. M. Dyke, J. Grigg, G. Herbert, W. Levason, G. McRobbie and G. Reid, *Inorg. Chem.*, 2023, **62**, 20844.
- 13 P. J. Blower, W. Levason, S. Luthra, G. McRobbie, F. M. Monzittu, T. O. Mules, G. Reid and M. N. Subhan, *Dalton Trans.*, 2019, **48**, 6767.
- 14 F. N. Penkert, T. Weyhermuller and K. Wieghardt, *Chem. Commun.*, 1998, 557.
- 15 K. S. Pedersen, G. Lorusso, J. J. Morales, T. Weyhermüller, S. Piligkos, S. K. Singh, D. Larsen, M. Schau-Magnussen, G. Rajaraman, M. Evangelisti and J. Bendix, *Angew. Chem., Int. Ed.*, 2014, **53**, 2394.
- 16 R. Bhalla, W. Levason, S. K. Luthra, G. McRobbie, G. Reid, G. Sanderson and W. Zhang, *Chem. Commun.*, 2014, **50**, 12673.
- 17 (a) D. Shetty, S. Y. Choi, J. M. Jeong, L. Hoigebazar, Y.-S. Lee, D. S. Lee, J.-K. Chung, M. C. Lee and Y. K. Chung, *Eur. J. Inorg. Chem.*, 2010, 5432–5438; (b) R. D. Hancock, H. Maumela and A. S. de Sousa, *Coord. Chem. Rev.*, 1996, **148**, 315.
- 18 T. Weyhermuller, K. Wieghardt and P. Chaudhuri, *J. Chem. Soc., Dalton Trans.*, 1998, 3805.
- 19 J. Huskens and A. Dean Sherry, *J. Chem. Soc., Dalton Trans.*, 1998, 177.
- 20 A. J. Blake, I. A. Fallis, A. Heppeler, S. Parsons, S. A. Ross and M. Schroder, *J. Chem. Soc., Dalton Trans.*, 1996, 31.
- 21 Z. Zhang, Y. He, Q. Zhao, W. Xu, Y.-Z. Li and Z.-L. Wang, *Inorg. Chem. Commun.*, 2006, **9**, 269.
- 22 S. Amin, C. Marks, L. M. Toomey, M. R. Churchill and J. R. Morrow, *Inorg. Chim. Acta*, 1996, **246**, 99.
- 23 P. B. Tsitovich and J. R. Morrow, *Inorg. Chim. Acta*, 2012, **393**, 3.
- 24 R. E. H. Kuveke, L. Barwise, Y. van Ingen, K. Vashisth, N. Roberts, S. S. Chitnis, J. L. Dutton, C. D. Martin and R. L. Melen, *ACS Cent. Sci.*, 2022, **8**, 855.
- 25 J. E. Richman and T. J. Atkins, *J. Am. Chem. Soc.*, 1974, **96**, 2268.
- 26 A. E. Martin, T. M. Ford and J. E. Bulkowski, *J. Org. Chem.*, 1982, **47**, 412.
- 27 L. Zhaowen, Z. Li, X. Chunfen, Y. Yong, Z. Fanbo and H. Kaixun, *Med. Chem. Res.*, 2007, **16**, 380.
- 28 R. Bhalla, J. Burt, A. L. Hector, W. Levason, S. K. Luthra, G. McRobbie, F. M. Monzittu and G. Reid, *Polyhedron*, 2016, **106**, 65.
- 29 R. Bhalla, W. Levason, S. K. Luthra, G. McRobbie, F. M. Monzittu, J. Palmer, G. Reid, G. Sanderson and W. Zhang, *Dalton Trans.*, 2015, **44**, 9569.
- 30 F. M. Monzittu, I. Khan, W. Levason, S. K. Luthra, G. McRobbie and G. Reid, *Angew. Chem., Int. Ed.*, 2018, **57**, 6658.
- 31 G. R. Giesbrecht, A. Gebauer, A. Shafir and J. Arnold, *Dalton Trans.*, 2000, 4018.

